EurJOC
European Journal of Organic Chemistry

A Journal of ChemPubSoc Europe

Accepted Article

Title: Synthesis of 6,6'-Bis(O-4-arylethynylbenzoyl)-α,α-Trehaloses and Their Utilization as Fluorescent Probes for Cellular Imaging

Authors: Kurumi Kobayashi, Rumiko Saito, Kaori Udagawa, Naoko Miyano-Kurosaki, Naoto Asano, Tetsuo Iwanaga, Naozumi Teramoto, Toshiaki Shimasaki, and Mitsuhiro Shibata

To be cited as: *Eur. J. Org. Chem.* 10.1002/ejoc.201800424

Link to VoR: http://dx.doi.org/10.1002/ejoc.201800424

Supported by ACES Asian Chemical Editorial Society

WILEY-VCH

10.1002/ejoc.201800424

Synthesis of 6,6'-Bis(*O*-4-arylethynylbenzoyl)-*α*,*α*-Trehaloses and Their Utilization as Fluorescent Probes for Cellular Imaging

Kurumi Kobayashi,[a] Rumiko Saito,[b] Kaori Udagawa,[b] Naoko Miyano-Kurosaki,[b] Naoto Asano,[c] Tetsuo Iwanaga,[c] Naozumi Teramoto,[a] Toshiaki Shimasaki,*[a] and Mitsuhiro Shibata*[a]

[a] Department of Applied Chemistry, Faculty of Engineering
Chiba Institute of Technology
Narashino, Chiba 275-0016, Japan
E-mail: tshima@sun.it-chiba.ac.jp and mitsuhiro.shibata@p.chibakoudai.jp
[b] Department of Life Science, Faculty of Advanced Engineering
Chiba Institute of Technology
Narashino, Chiba 275-0016, Japan
[c] Department of Chemistry, Faculty of Science
Okayama University of Science
1-1 Ridaicho, Kita-ku, Okayama 700-0005, Japan

Received ### 00, 2018

Graphical Abstract

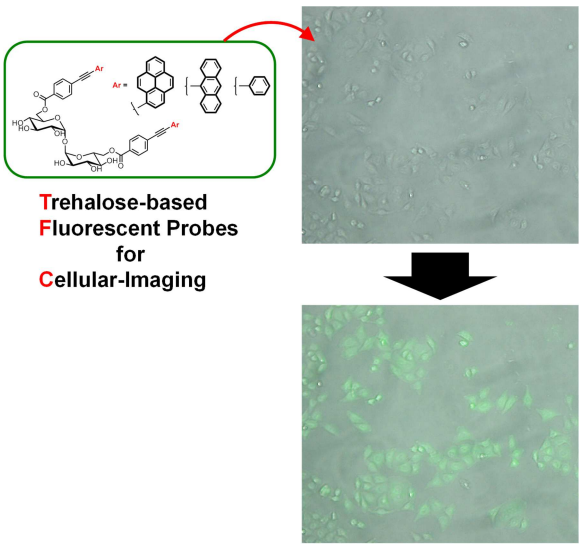

6,6'-Bis(*O*-4-arylethynylbenzoyl)-*α*,*α*-trehaloses **1a**, **1b** and **1c** (aryl = 1-pyrenyl, 9-anthryl and phenyl, respectively) were synthesized, and their photophysical properties were examined by UV-vis and fluorescence spectroscopies in anhydrous or hydrous THF solutions. Especially, the pyrenyl derivative **1a** acted as an excellent fluorescent probe for cytofluorometric imaging.

Abstract

A series of 6,6'-bis(*O*-4-arylethynylbenzoyl)-*α*,*α*-trehaloses (aryl groups; **1a**: 1-pyrenyl, **1b**: 9-anthryl, **1c**: phenyl) were synthesized and fully characterized. Their photophysical properties were investigated by UV-vis/fluorescence spectroscopies, and were rationalized by TDDFT calculations. Moreover, the emission maxima of **1a** and **1b** in THF/H_2O considerably shifted to a longer wavelength region with increasing H_2O fraction owing to the formation of excimers. The pyrenyl derivative **1a** was efficiently taken into HeLa $CD4^+$ human cervical cancer cells and emitted bright green fluorescence.

Keywords: Fluorescent probe, Cellular imaging analysis, Trehalose, Fused aromatics, Photophysical properties

1. Introduction

Fused aromatic compounds possessing π-conjugated substituents have been gathering much attention as photo functional materials such as organic solar cells,[1] organic light-emitting diodes (OLEDs)[2] and organic field-effect transistors (OFETs)[3] due to their high fluorescent quantum yields.[4] The extension of π-conjugation can be attained by fusing aromatic rings and/or introducing π-bridges. The elongation of π-conjugation generally provides electron-rich aromatics with a highly fluorescent character. For example, Rashatasakhon and co-workers reported a novel C_3 symmetrical truxane derivative with three ethynylpyrene pendants in 2014.[5] This π-electron abundantly truxane derivative displayed the good emission properties with high quantum yield even in aqueous THF, and it was successfully applied to the sensing of picric acid with a detection limit of 0.15 ppm. Thus, the aromatic compounds having large π-conjugation can be used for the chemical sensors by using their highly fluorescent character.[6] Moreover, Vicente and co-workers recently reported the synthesis and spectroscopic and cellular properties of aryl-fused 4,4-difluoro-4-bora-3a,4a-diaza-*s*-indacenes (BODIPYs).[7] In this paper, they reported that

[*α*]phenanthrene-fused BODIPYs strongly absorb and emit in a near-IR region (641−701 nnm), and can be applied to bio-imaging agents in human HEp2 cells. Thus, the compounds having fused aromatic structure and/or π-bridge are good candidates of fluorescent probes[8] as well as organic electronic functional materials. As examples of the cellular imaging by combining sugars and fluorescent aromatic compounds, Laughlin, Baskin and co-workers reported in vivo imaging of membrane-associated glycans as follows: Zebrafish embryos were treated with peracetylated *N*-azidoacetylgalactosamine; subsequently, the embryos were reacted with a difluorinated cyclooctyne containing Alexa Fluor 555 (a derivative of 3,6-diaminoxanthene-4,5-disulfate) cadaverine as a fluorophore; enabling the visualization of glycans in vivo at subcellular resolution during development.[9] Also, Hsu and co-workers reported that the azide-alkyne click chemistry of 3-azido-7-hydoxycoumarin with the cellular glycans, in which peracetylated alkynyl fucose and *N*-acetylmannosamine were incorporated as fluorescent molecules, is an effective method for the labeling and visualization of glycoconjugates in cells.[10] Barattucci, Sciortino, Puntoriero and coworkers reported that a dimethylamino-substituted oligo(phenylene-ethynylene) glucoside acts as an efficient biocompatible fluorescent cell probe.[11] Moreover, Ribagorda, Barattucci and co-workers reported that the dimethylamino-oligo(phenylene-ethynylene) glucoside derivatives are applicable to photosensitizers in photodynamic therapy by using their photophysical properties such as high quantum yield, singlet oxygen production, bio-compatibility, stability, easy cell-internalization and very good response.[12] Thus, it is expected that the compounds prepared by combining fluorescent aromatic compounds with sugars are promising fluorescent probes for cellular imaging.

Trehalose has two glucose moieties linked together by an *α*,*α*-1,1'-glycoside bond between those anomeric carbons, therefore it is a non-reducing disaccharide.[13] Trehalose exists abundantly in nature and it is widely used in food and cosmetics. As an example of glycolipids possessing trehalose moieties, maradolipid, which is a dissymmetrically 6,6'-di-*O*-acylated trehalose, was isolated from *C. elegans*.

Maradolipid is also known to show diverse immune activities, and it was chemically synthesized by Kulkarni and Knölker independently.[14] Glycolipids play an important role to maintain the stability of the cell membrane and to facilitate cellular recognition, which is crucial to the immune response and in the connections that allow cells to connect to one another to form tissues. For instance, very recently, Timmer and Stocker synthesized 6,6'-bis(*O*-fatty acyl)trehaloses with linear and iso-branched alkyl chains, and determined that these trehalose diesters activate macrophages in a Mincle-dependent manner.[15]

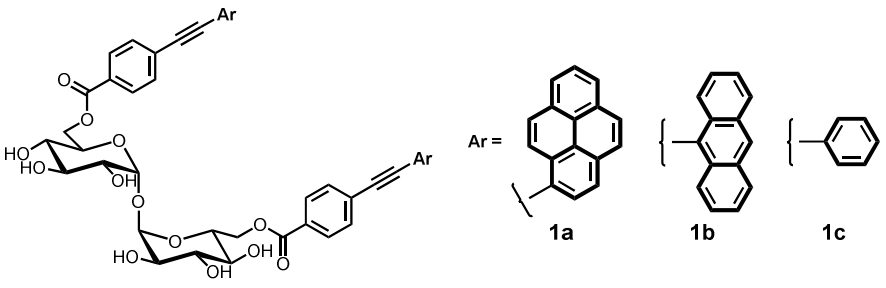

Figure 1. Structure of 6,6'-bis(*O*-4-arylethynylbenzoyl)-*α*,*α*-trehaloses **1a**−**1c**.

As described above, the biological compatibility of trehalose and intense fluorescent character of fused aromatic compounds led us to design a series of 6,6'-bis(*O*-4-arylethynylbenzoyl)-*α*,*α*-trehaloses **1a**−**1c** possessing 1-pyrenyl, 9-anthryl and and phenyl as aryl groups (Figure 1). Especially, it is expected that pyrenyl and anthryl derivatives **1a** and **1b** are excellent candidates of fluorescent probes for cellular imaging, considering that 1-phenylethynylpyrene and 9-phenylethylanthracene exhibits the intense fluorescence and very high quantum yield.[16] In this study, aryl-substituted trehaloses **1a**−**1c** were successfully synthesized, and their structural and photophysical properties were investigated in detail. Furthermore, based on the photophysical properties, pyrenyl derivative **1a** was examined as a fluorescent probe for *in vitro* imaging of HeLa $CD4^+$ human cervical cancer cells. Consequently, **1a** acted as an excellent fluorescent probe for cytofluorometric imaging.

Synthesis.

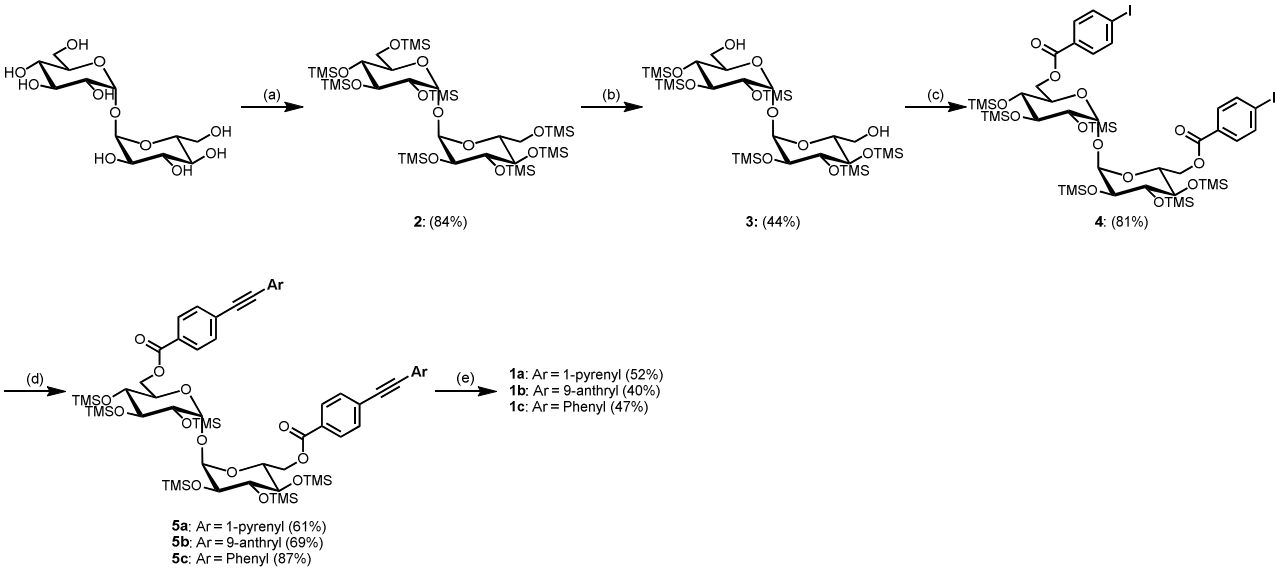

Scheme 1. Synthesis of 6,6'-bis(*O*-4-arylethynylbenzoyl)-α,α-trehaloses **1a**−**1c**. Reagents and conditions: (a) trimethylsilyl chloride, Et_3N/CH_2Cl_2 (1:1 v/v), 0°C, 24 h; (b) K_2CO_3 (0.5 mol eq.), CH_2Cl_2/MeOH (1:3 v/v), 0°C, 1h; (c) 4-iodobenzoic acid (3.0 mol eq.), DCC (3.0 mol eq.), DMAP (0.3 mol eq.), CH_2Cl_2, rt, 24 h; (d) **a**: 1-ethynylpyrene (4.0 mol eq.), **b**: 9-ethynylanthracene (4.0 mol eq.), **c**: ethynylbenzene (4.0 mol eq.), $PdCl_2(PPh_3)_2$ (0.2 mol eq.), CuI (0.2 mol eq.), THF/NEt_3 (3:1 v/v), rt, 48 h; (e) TBAF (7.2 mol eq.), THF, rt, 1h. DCC = *N*,*N*'-dicyclohexylcarbodiimide, DMAP = 4-dimethylaminopyridine, TBAF = tetrabutylammonium fluoride.

The synthetic route for bis(*O*-arylethynylbenzoyl)trehaloses **1a**, **1b** and **1c** is outlined in Scheme 1. 2,3,4,2',3',4'-hexakis(*O*-trimethylsilyl)trehalose **3** was synthesized according to a known procedure[14b] via the selective deprodection reaction of trimethylsilyl (TMS) groups of per(*O*-trimethylsilyl)trehalose **2** in an overall yield of 37% from trehalose. Dihydroxy compound **3** was esterificated by 4-iodobenzoic acid to afford a bis(iodophenyl) derivative **4** (81%). The key intermediate **4** was coupled with three kinds of aryl acetylenes (Ar = 1-pyrenyl, 9-anthryl and phenyl) prepared from the corresponding aryl halides, to give compounds **5a**−**5c** in a modest to good yield (**5a**: 61%, **5b**: 69%, **5c**: 87%). At last, six TMS groups of **5a**−**5c** were de-protected by tetrabutylammonium fluoride (TBAF) in THF to generate objective compounds **1a**−**1c** (**1a**: 52%, **1b**: 40%, **1c**: 47%). The arylethynyl-substituted trehaloses **1a**−**1c** were fully characterized by using various analytical techniques such as ^1H and ^{13}C NMR, FT-IR spectroscopies and high

resolution mass spectrometry.

Molecular structure.

Bis(*O*-arylethynylbenzoyl)trehaloses **1a**−**1c** were soluble in high-polar solvents and cyclic ethers such as DMSO, DMF, dimethylacetoamide (DMA), dioxane and THF, while insoluble in CH_2Cl_2, $CHCl_3$, methanol, ethanol, isopropylalcohol, acetone, EtOAc, diethylether and hexane. Although we tried the recrystallization of **1a**−**1c** with dioxane or THF, we could not get their single crystals. Therefore, the structural properties of compounds **1a**−**1c** were determined by DFT calculations at the B3LYP /6-31G(d) level of theory.

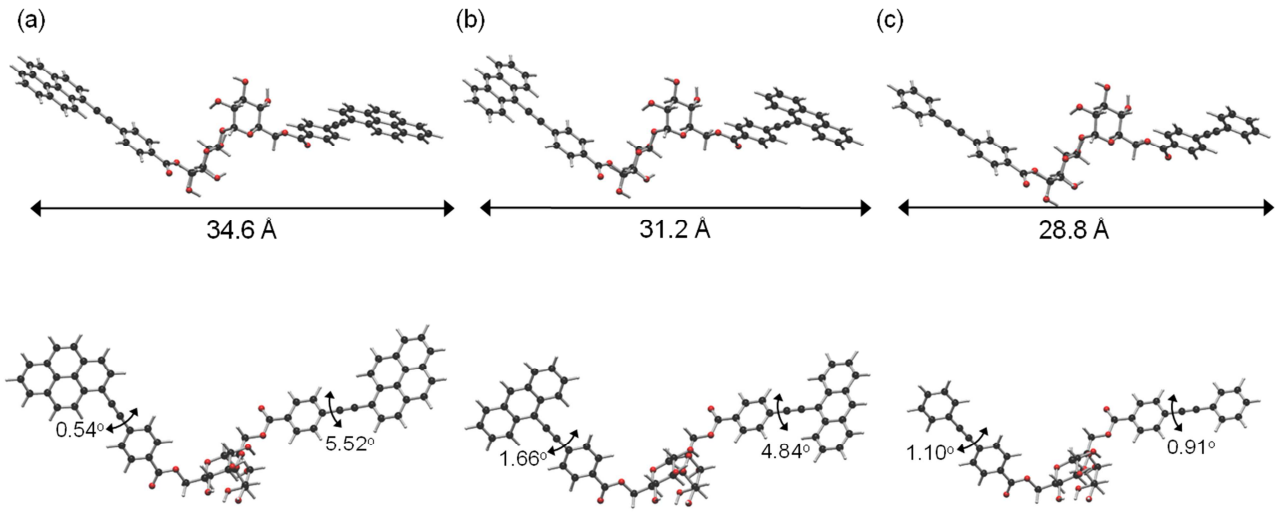

Figure 2. Calculated structures of a) compound **1a**; b) compound **1b**; c) compound **1c** at the B3LYP/6-31G(d) level of theory. The lower structures represent the top view and the upper structures represent side view, respectively.

The calculated structures of compounds **1a**−**1c** were shown in Figure 2. The calculated bond lengths of two C≡C bonds (1.22 Å) in each compound were almost identical to a typical C≡C bond length. Two ethynylene-bridged 1-pyrenyl and phenylene moieties of compound **1a** were slightly twisted by 0.54 and 5.52°. Also, the torsional angles between two ethynylene-bridged 9-anthryl and phenylene moieties of **1b** were 1.66 and 4.84°. In the case of compound **1c**, the torsional angles between two pairs of benzene rings

were 1.10 and 0.91°, indicating that the steric hindrance is alleviated in comparison with **1a** and **1b**. Thus, DFT calculation revealed that each terminal arylethynylphenyl moiety of **1a**−**1c** is somewhat deviated from a planar structure. These arylethynylphenyl moieties were located far apart from each other as shown at the top of Figure 2. End-to-end distances between terminal two aryl groups for **1a**, **1b** and **1c** were 34.6, 31.2 and 28.8 Å, respectively. On the other hand, the distances of OH−O for **1a** (2.13−2.46 Å), **1b** (2.13−2.47 Å) and **1c** (2.13−2.46 Å) in trehalose moiety were shorter than the sum of van der Waals radii (2.72 Å) of hydrogen (1.20 Å) and oxygen (1.52 Å). Therefore, all hydroxy groups of trehalose for **1a**, **1b** and **1c** can be considered to form the intramolecular multi hydrogen bonds. Such intramolecular multi hydrogen bonds strongly indicate that the trehalose takes the rigid conformation. These results of DFT calculations exhibit that the hydrophobic and hydrophilic moieties for **1a**−**1c** are located on the periphery and center of molecular structure, respectively.

Electronic Absorption Spectroscopy.

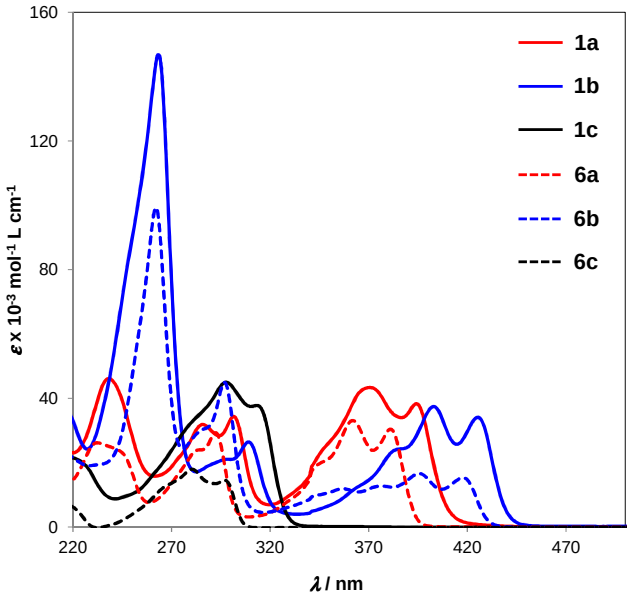

Figure 3. Electronic absorption spectra of bis(*O*-arylethynylbenzoyl)trehaloses **1a**−**1c** and their reference compounds **6a**−**6c** in THF at 298 K.

Table 1. UV-vis spectral data of **1a**−**1c** and **6a**−**6c**, and theoretical calculated lowest absorption maxima[a,b]

	λ_{max}^{abs} [nm] (eV)	ε [M^{-1} cm^{-1}]	calcd λ_{max}^{abs} [nm] (f)[b]	composition of band of calcd λ_{max}^{abs} [b]
1a	238 (5.21)	46,100	407 (1.502)	H → L+1, 55%
	286 (4.34)	31,900		H−1 → L, 42%
	302 (4.11)	34,200		
	370 (3.35)	43,300		
	395 (3.14)	38,100		
1b	263 (4.71)	146,700	443 (0.739)	H → L+1, 64%
	294[c] (4.22)	20,400		H−1 → L, 35%
	309 (4.01)	26,400		
	384[c] (3.23)	24,100		
	403 (3.08)	37,400		
	425 (2.92)	34,100		
1c	220 (5.64)	21,600	319 (1.694)	H → L+1, 61%
	298 (4.16)	44,900		H−1 → L, 37%
	313 (3.96)	37,800		
6a	232 (5.34)	26,100	387 (0.838)	H → L, 97%
	242[c] (5.12)	24,200		
	292[c] (4.25)	29,200		
	343 (3.62)	18,700		
	362 (3.43)	33,100		
	381 (3.25)	30,400		
6b	262 (4.73)	99,300	431 (0.339)	H → L, 99%
	297 (4.18)	44,900		
	374[c] (3.32)	12,600		
	396 (3.13)	16,600		
	418 (2.97)	15,300		
6c	280 (4.43)	17,900	294 (0.930)	H → L, 97%
	297 (4.18)	14,500		H−3 → L+4, 3%

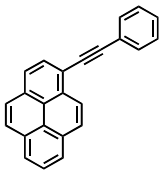
6a

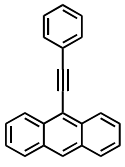
6b

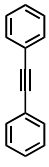
6c

[a]in THF. [b]The data were afforded by time-dependent (TD) DFT calculations of **1a**−**1c** and **6a**−**6c** at the B3LYP/cc-pVDZ // B3LYP/6-31G(d) level of theory using the optimized structures.; f = oscillator strength. H = HOMO, L = LUMO. [c]Peak as a shoulder.

To investigate the basic photophysical properties of **1a**−**1c**, the UV/Vis absorption spectra of dilute

solutions in THF (1×10^{-5} M) at 298 K were compared with those of 1-phenylethynylpyrene **6a**, 9-phenylethynylanthracene **6b** and phenylethynylbenzene **6c** as reference compounds (Figure 3). Table 1 summarizes their experimental spectral data as well as time-dependent (TD) DFT results at the B3LYP/cc-pVDZ // B3LYP/6-31G(d) . The absorption spectrum of dipyrenyl compound **1a** was mainly composed of three bands, among which the highest energy band was located at 238 nm. The second band for **1a** had two peaks at 286 and 302 nm, and the third band (λ_{max}^{abs}) also had two peaks at 370 and 395 nm. The dianthryl compound **1b** also exhibited a similar spectral pattern to that of **1a**. The highest energy band of **1b** was located at 263 nm and the second one was at 309 nm with a shoulder at around 294 nm. The third one was composed of two peaks at 403 and 425 nm, which was observed at a lower energy region than a typical α-absorption band of anthracene by the π-conjugation through ethynylene bridges. On the other hand, the spectrum of **1c** was quite simple, and mainly two curves appeared at around 220 and 300 nm. The molar absorption coefficients (ε) for **1a** and **1b** (**1a**: 46,100 (238 nm), **1b**: 146,700 (263 nm)) were approximately 1.5 times larger than those of the corresponding reference compounds **6a** and **6b** (**6a**: 26,100 (232 nm), **6b**: 99,300 (262 nm)).

The fact that the absorption terminals of **1a** and **1b** reached to a visible region means that visible light can be used for excitation when these compounds are introduced into cell. On the other hand, the longest λ_{max}^{abs} of compound **1c** appeared at 313 nm, which was located at a considerably shorter wavelength region than those of **1a** and **1b**.

Fluorescence Spectroscopy.

10.1002/ejoc.201800424

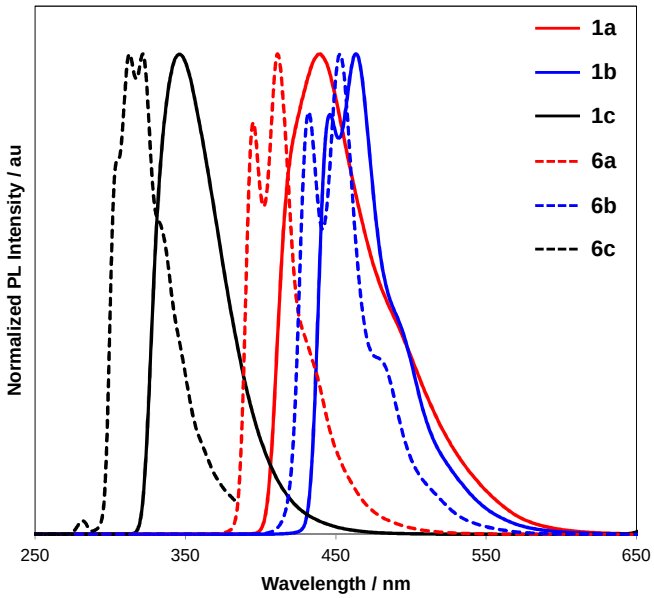

Figure 4. Fluorescence spectra of bis(*O*-arylethynylbenzoyl)trehaloses **1a**−**1c** and their reference compounds **6a**−**6c** in THF at 298 K.

Table 2. Fluorescence data of **1a**−**1c**.[a]

	λ_{max}^{abs} [nm] (in THF)	λ_{ex} [nm]	λ_{max}^{fl} [nm] (in THF)	ν_{ST} / cm^{-1}[b]	Φ_f[d]
1a	395	395	439	2,537	0.91
			498[c]		
1b	425	425	446	1,108	0.76
			463	1,931	
1c	313	313	346	3,047	0.42
6a	381	381	395	930	0.79
			411	1,916	
6b	418	418	432	775	0.84
			453	1,848	
6c	297	297	313	1,721	n.d.
			322	2,614	

[a]Measured at 1×10^{-5} M in THF. [b]Stokes shift. [c]Peak as a shoulder. [d]Absolute quantum yields were determined by an integrating sphere system.

As described above, it is well known that fused aromatic compounds such as pyrene and anthracene derivatives generally show a fluorescent character. Actually, not only fused aromatic compounds **1a** and **1b**, but also monocyclic aromatic compound **1c** exhibited intense fluorescence character in diluted THF solutions

(1×10^{-5} M) as shown in Figure 4. The fluorescent maximum (λ_{max}^{fl}) for compound **1a** was observed as a broad peak having no vibrational structure at 439 nm, which was in a longer wavelength region than that of the reference compound **6a** (411 nm). Furthermore, the emission band contained a shoulder peak at around 500 nm as shown in Figure 4. When the fluorescent spectrum was measured in more diluted concentration (1×10^{-6} M), the shoulder was not appeared in spectral band (see Figure *S*22 and Table *S*1). Also, the total spectral shapes of **1a** between 1×10^{-5} M and 1×10^{-6} M were substantially different from each other. Hence, we assigned that this shoulder peak shown in Figure 4 would be derived from an intermolecular excimer (excited dimer) emission band. On the other hand, it is inferred that the excimer emission is not formed for **1b**, because there was little difference in the spectral shape with the vibrational structure between **1b** (λ_{max}^{fl} = 463 nm) and **6b** (λ_{max}^{fl} = 453 nm). Additionally, the total spectral shape was also almost no changed between 1×10^{-5} M and 1×10^{-6} M (see Figures 4 and *S*22). Although the Storks shift (ν_{ST}) of **1c** (3,047 cm^{-1}) was relatively large compared with those of **1a** (2,537 cm^{-1}) and **1b** (1,931 cm^{-1}), it was observed still in a UV region (λ_{max}^{fl} = 346 nm). Table 2 also summarizes absolute fluorescent yields (Φ_f) of **1a**−**1c** and **6a**−**6c** determined by an integrating sphere system. The Φ_f values of fluorescent probes **1a**−**1c** were 0.91 (**1a**), 0.76 (**1b**) and 0.42 (**1c**), these values were comparable to or higher than those (**6a**: 0.79, **6b**: 0.84. **6c**: n.d.) of reference compounds **6a**−**6c** with no hydrophilic moieties. The higher orders of Φ_f values were **1a** > **1b** > **1c** for **1a**−**c**, and **6a** > **6b** > **6c** for **6a**−**c**.

10.1002/ejoc.201800424

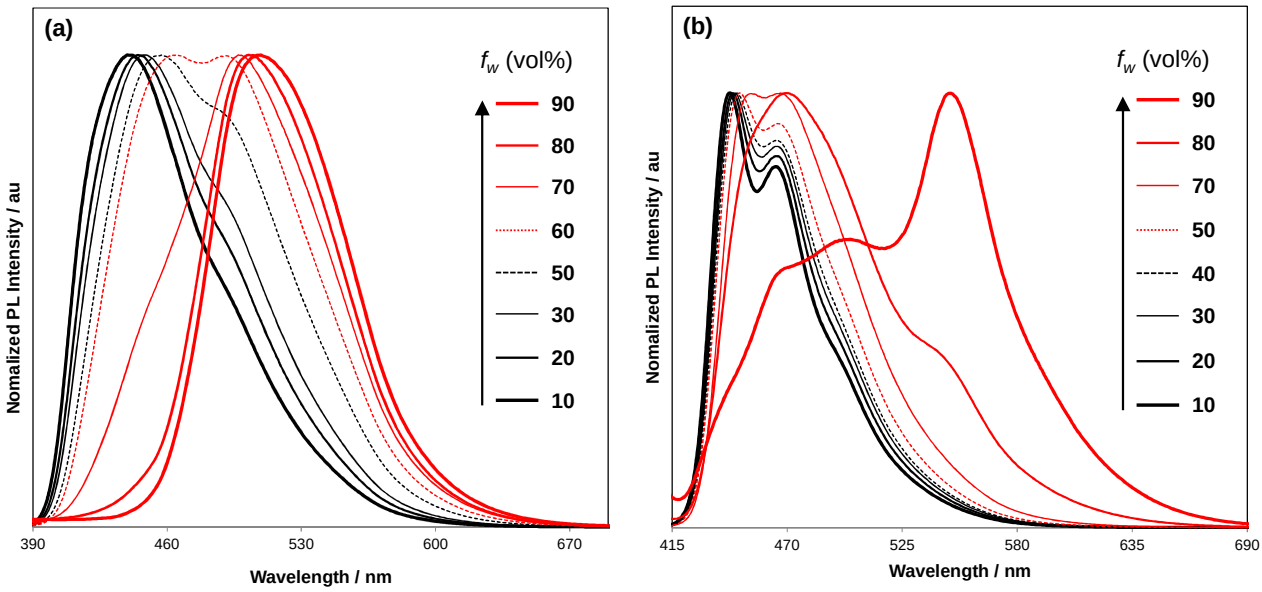

Figure 5. Fluorescence spectra of **1a** (a) and **1b** (b) in THF/water mixtures with different water fractions (f_w) at 298 K.

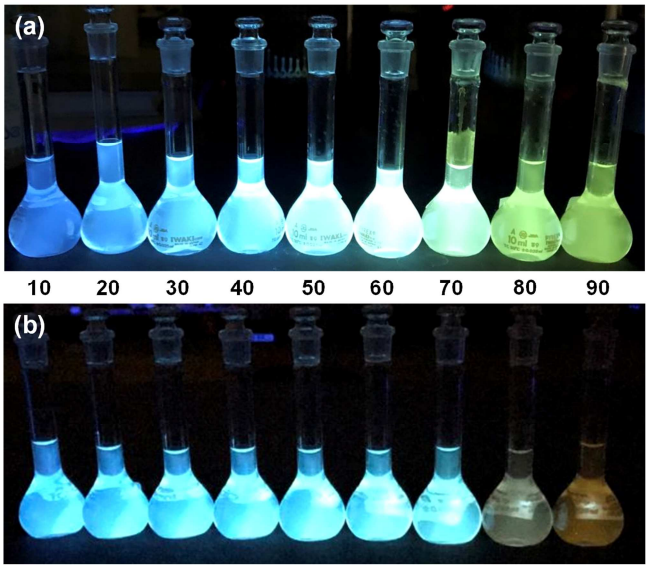

Figure 6. The fluorescence photographs of **1a** (a) and **1b** (b) in THF/H_2O mixtures with different water fractions (f_w).

Table 3. Fluorescence data of **1a** and **1b** in THF/ H_2O mixtures with different H_2O fractions (f_w).[a]

f_w (THF/H_2O)	λ_{max}^{fl} [nm] for **1a**	$\lambda_{max}^{fl} - \lambda_0^{fl}$ cm^{-1} [b] **1a**	Φ_f [c] for **1a**	λ_{max}^{fl} [nm] for **1b**	$\lambda_{max}^{fl} - \lambda_0^{fl}$ cm^{-1} [b] **1b**	Φ_f [c] for **1b**
100/0	439	–	0.91	443	–	0.76
				463	–	
90/10	440	51.8	–	443	0	–
				465	92.9	

80/20	445	307	–	444	50.8	–
				465	92.9	
70/30	449	507	–	445	102	–
				465	92.9	
60/40	449	507	–	446	152	–
				465	92.9	
50/50	457	897	–	447	202	–
				465	92.9	
40/60	465	1,274	0.72	449	302	0.45
	491	2,412		467	92.1	
30/70	497	2,658	–	453	498	–
				467	92.1	
20/80	506	3,016	–	470	322	–
				543[d]	3,089	
10/90	509	3,033	0.31	468[d]	1,206	0.02
				500	1,598	
				548	3,350	

[a]Measured at 1×10^{-5} M in THF with different H_2O fractions. [b]λ_0^{fl} is λ_{max}^{fl} of **1a** and **1b** in THF. [c]Absolute quantum yields were determined by an integrating sphere system. [d]Peak as a shoulder.

In the fluorescence spectra of compound **1a** and **1b** measured in THF/H_2O mixtures with different H_2O fractions (Figure 5), the values of λ_{max}^{fl} for **1a** and **1b** became longer with increasing H_2O fraction. The fluorescent curves of **1a** in THF/H_2O 40/60 and **1b** in THF/ H_2O 30/70 were composed of two peaks at 465 and 491 nm, and 449 and 467 nm, respectively. When the ratio of THF/H_2O is 10/90 for **1a**, the fluorescent band became a broad peak at 509 nm, and the value of $\lambda_{max}^{fl} - \lambda_0^{fl}$ was 3,033 cm^{-1} (Table 3). Thus, when the water fraction was increased for **1a**, the original fluorescent emission band gradually disappeared, and the shoulder band shifted to a longer wavelength region. It is inferred that the spectral change for **1a** is derived from the excimer, which is formed by the aggregation of hydrophobic 1-phenylethynylpyrenyl moieties of **1a** by the addition of H_2O.[17] Also, the longest emission band of **1b** shifted to 548 nm in THF/H_2O 10/90, and the value of $\lambda_{max}^{fl} - \lambda_0^{fl}$ was 3,350 cm^{-1}. In order to play a role as a highly efficient cellular fluorescent probe, the broad emission band is quite important.[11] When **1a**–**1c** are used as a fluorescent probe in a living

cell, it is also quite important to elucidate the water content-dependency of fluorescent spectra, because it is necessary to generate fluorescent light in a H_2O-rich condition. Therefore, we measured fluorescent yields (Φ_f) of **1a** and **1b** in the THF/H_2O ratios of 40/60 and 10/90 by an integrating sphere system. The Φ_f values (0.31 and 0.02) of **1a** and **1b** in THF/H_2O 10/90 were much smaller than those (0.72 and 0.45) in THF/H_2O 40/60. We confirmed that **1a** exhibits a green color emission due to the excimer formation in THF/H_2O 10/90, whereas **1b** almost did not emit light in the H_2O-rich condition, as is obvious from Figure 6.

Computational Analysis.

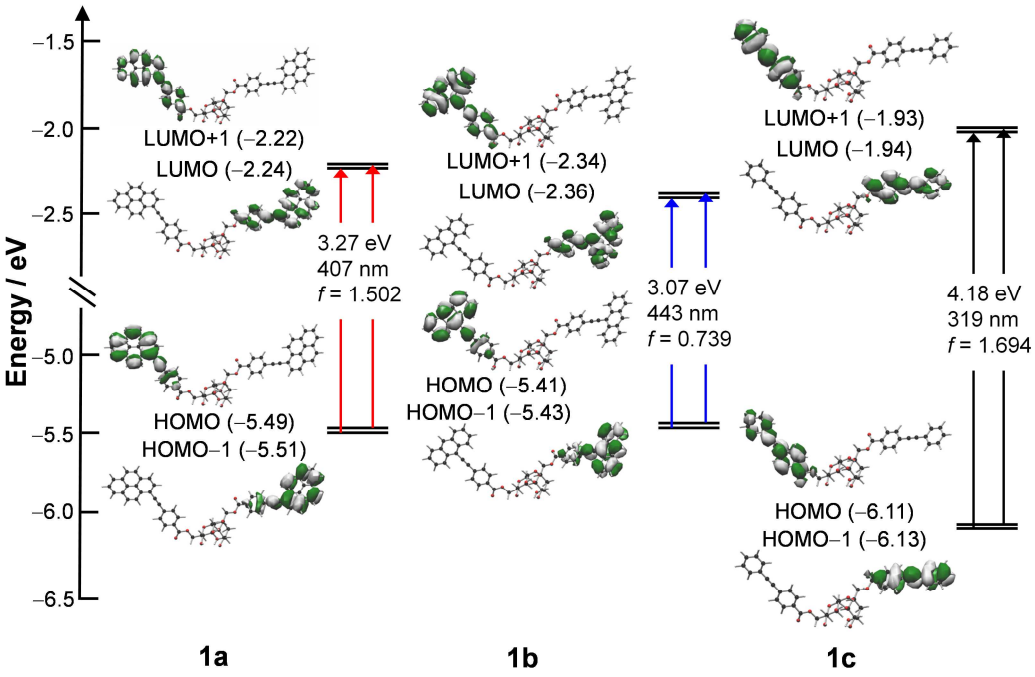

Figure 7. Calculated FMO orbitals for **1a**−**1c** and their transition properties at the B3LYP/cc-pVDZ // B3LYP/6-31G(d) level of theory.

The time-dependent (TD) DFT and single point calculations using global minimum optimized structures for compounds **1a**−**1c** and **6a**−**6c** were performed at the B3LYP/cc-pVDZ // B3LYP/6-31G(d) level of theory to obtain some insights into the electronic properties. As shown in Figure 7, the HOMO and LUMO

orbitals of each compound were spread on the aromatic and ethynylene moieties. Especially, the LUMO orbital of each compound was also located at a carbonyl group beyond the connected ethynylene bridge. The fact that λ_{max}^{abs} values of **1a**−**1c** were a little longer than those of reference compounds **6a**−**6c** can be explained by a decrease of the HOMO−LUMO gap due to the LUMO stabilization.

The transition properties of the longest λ_{max}^{abs} for compounds **1a**−**1c** were elucidated by TDDFT calculations at the B3LYP/cc-pVDZ level. As described in Table 1 and Figure 7, the absorption maxima of compounds **1a**−**1c** are based on the transitions from HOMO−1 to LUMO and from HOMO to LUMO+1. The calculated longest λ_{max}^{abs} of 9-ethynylanthryl compound **1b** was 443 nm, which was in good agreement with the experimental value. The fact that the calculated longest λ_{max}^{abs} (407 nm) of 1-ethynylpyrenyl compound **1a** was shorter by 36 nm than that of **1b** is caused by the lowering of the LUMO level of **1b**. On the other hand, the HOMO−LUMO gap of ethynylphenyl compound **1c** was larger than those of **1a** and **1b**, reflecting that **1c** have no fused aromatic rings.

Cellular Imaging Study.

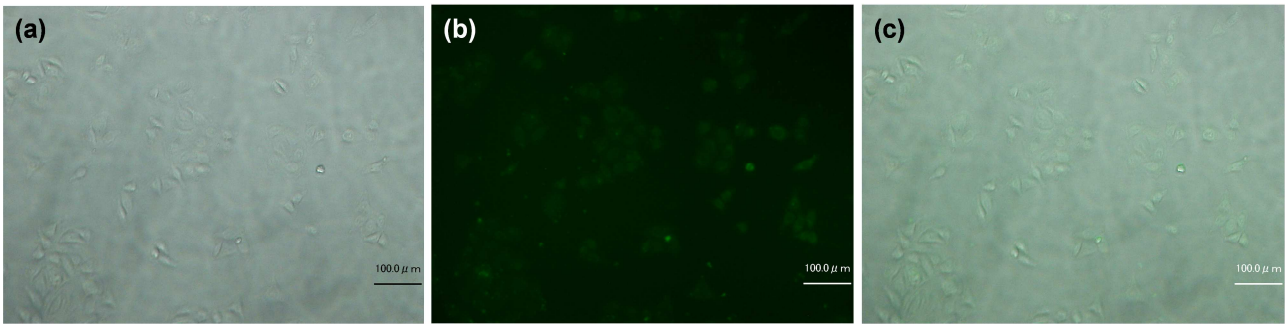

Figure 8. (a) Bright field image, (b) Fluorescence image (490 nm excitation, 520−530 nm emission range), (c) Overlay image of HeLa $CD4^+$ cells in presence of **1a** (15.0 μM).

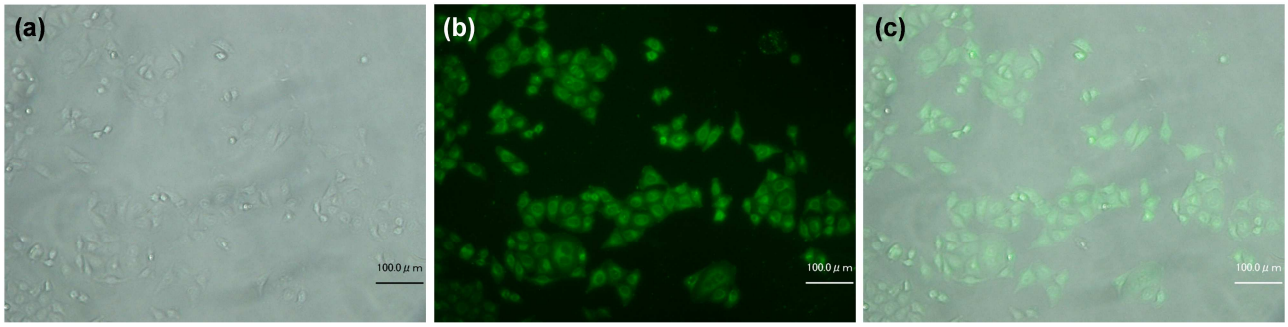

Figure 9. (a) Bright field image, (b) Fluorescence image (490 nm excitation, 520−530 nm emission range), (c) Overlay image of HeLa $CD4^+$ cells in presence of **1a** (37.5 μM).

Based on the experimental and calculated results of photophysical properties for compounds **1a**−**1c**, we performed an uptake study into HeLa $CD4^+$ human cervical cancer cells using **1a** as a green color fluorescent probe. The cells were cultivated on D-MEM basal media with 10μL of **1a** (37.5 μM in DMSO/PBS 80/20), 10% FBS and penicillin/streptomycin at 37°C under air condition including 5%CO_2 for 24 h. The pyrenyl compound **1a** was successfully taken into the HeLa $CD4^+$ cells (Figure 9 (a) and (b)), even when cells are incubated at low concentrations of up to 15.0 μM (Figure 8 (a) and (b)). It was demonstrated that the pyrenyl compound **1a** in the HeLa $CD4^+$ cells emitted bright green luminescence when excited by 490 nm visible light. The luminescence was the same color as the luminescence (520−530 nm) of **1a** in THF/H_2O 10/90. Moreover, in order to examine the bio-compatibility of fluorescent probe **1a**, we performed the cell viability tests by using DMSO/PBS (80/20) solutions of **1a** as shown in Figure S23. Consequently, the averages of cell viabilities in various concentrations were 48−64% after 24 h, and were almost the same as the case of only DMSO/PBS (60%). These results strongly suggest that the modest cell viabilities are caused by the toxicity of DMSO. Thus, we clarified that pyrenyl derivative **1a** was efficiently taken toward the HeLa $CD4^+$ cells, and served as a green color cell imaging probe.

Conclusions.

In summary, we synthesized a series of new aryl-substituted trehaloses **1a**−**1c** via the TMS-protection of hydroxy

groups of trehalose, selective deprotection, esterification of two primary hydroxy groups and Sonogashira cross-coupling reactions. The structural features of **1a**−**1c** were investigated by DFT calculations at the B3LYP/6-31G(d) level of theory. The UV-vis spectral analysis for **1a**−**1c** revealed that pyrenyl and anthryl derivatives **1a** and **1b** have absorption maxima in a visible region, while phenyl derivative **1c** does not. The compounds **1a**−**1c** emitted intense fluorescence at 313−415 nm in diluted THF solutions, and had high quantum yields (**1a**: 0.91, **1b**: 0.76, **1c**: 0.42). Although **1b** almost did not emit light in THF/H_2O 10/90 (Φ_f = 0.02), **1a** emitted a relatively intense fluorescence character even in THF/H_2O 10/90 (Φ_f = 0.31). It was demonstrated that pyrenyl derivative **1a** acts as a fluorescent probe having bright green emission, when it was introduced into the HeLa $CD4^+$ cells. The investigation of the second generation trehalose-based fluorescent probes is underway in our laboratory.

Experimental Section.

General experimental methods

All of the chemicals and solvents were purchased from commercial sources and used without further purification unless otherwise stated. Column chromatography and plug filtrations were performed on silica gel 60. TLC was performed on aluminum sheets that were coated with silica gel 60 F_{254}; visualization was performed with a lamp (λ = 254 or 365 nm). Melting points are uncorrected. IR spectra were recorded by using the attenuated total reflectance (ATR) method. UV/Vis spectra were recorded in a quartz cell (width: 10 mm). The UV/Vis and fluorescence spectra were measured in a cuvette of 1 cm at 298 K. The absorption maxima (λ_{max}^{abs}) are reported in nm, and the relative intensities or molar extinction coefficients are given in parentheses. Shoulders are denoted as sh. Absolute quantum yields were determined by using a calibrated integrating-sphere system in THF and THF/H_2O. Spectroscopic grade THF and H_2O was deaerated under ultrasound irradiation for 10 min just prior to use. NMR spectra were measured in $CDCl_3$ and DMSO d_6. Chemical shifts (δ) are given in ppm relative to tetramethylsilane (TMS). Coupling constants (J) are given in Hz. The apparent resonance multiplicity is described as s (singlet), d (doublet), t

(triplet), q (qualtet), quin (quintet), sep (septet) and m (multiplet). HRMS was performed for solutions in DMSO/MeCN on APCI mass spectrometers. All the theoretical calculations were performed by using the Gaussian program package.[18] The geometry optimizations were performed by the Becke's three-parameter hybrid functional (B3),[19] the Lee, Yang, and Parr (LYP) correlation,[20,21] and the 6-31G(d) Pople basis set.[22] TD calculations were performed by using the correlation consistent cc-pVDZ basis set of Dunning.[23]

Synthesis of compounds 1a−1c, 3, 4, 5a−5c and 6a

2,3,4,2',3',4'-Hexakis(*O*-trimethylsilyl)-*α*,*α*-trehalose (3)

2,3,4,2',3',4'-Hexakis(*O*-trimethylsilyl)-*α*,*α*-trehalose **3** was synthesized according to the reported manner.[14b] All spectral data were completely identical with the reported data.

1-(Phenylethynyl)pyrene (6a)

1-(Phenylethynyl)pyrene **6a** was synthesized according to the previous literature.[24] All spectral data were completely identical with the reported data.

6,6'-Bis(*O*-4-iodobenzoyl)-2,3,4,2',3',4'-hexakis(*O*-trimethylsilyl)-*α*,*α*-trehalose (4)

Under a nitrogen atmosphere, DCC (1.98 mL, 8.82 mmol) and DMAP (110.2 mg. 0.880 mmol) was added into a solution of 2,3,4,2',3',4'-hexakis(*O*-trimethylsilyl)-*α*,*α*-trehalose **3** (2.28 g, 2.94 mmol) and 4-iodobenzoic acid (2.19 g, 8.82 mmol) in CH_2Cl_2 (40 mL) at room temperature. After stirring for 48h, the white powder was removed by filtration, and the solvent was removed under reduced pressure. The residual mixture was purified by flash column chromatography on silica gel (*n*-hexane/AcOEt, 19:1) to give 6,6'-bis(*O*-4-iodobenzoyl)-2,3,4,2',3',4'-hexakis(*O*-trimethylsilyl)-*α*,*α*-trehalose **4** as a white powder. Yield,

2.95 g (2.39 mmol), 81%; mp, 139.5−140.5°C; ^{1}H NMR (500 MHz, $CDCl_3$) δ 0.12 (18H, s), 0.14 (18H, s), 0.18 (18H, s), 3.48 (2H, dd, *J* = 3.1 and 9.4 Hz), 3.61 (2H, t, *J* = 8.8 Hz), 3.96 (2H, t, *J* = 8.9 Hz), 4.11 (2H, dt, *J* = 3.2 and 9.2 Hz), 4.27 (2H, dd, *J* = 3.7 and 12.0 Hz), 4.56 (2H, dd, *J* = 2.5 and 12.1 Hz), 4.95 (2H, d, *J* = 3.1 Hz), 7.75 (4H, d, *J* = 8.7 Hz), 7.82 (4H, d, *J* = 8.7 Hz); ^{13}C NMR (125 MHz, $CDCl_3$) δ 0.25, 0.89, 1.07, 63.9, 70.8, 71.9, 72.7, 73.6, 94.5, 100.9, 129.5, 131.1, 137.8, 165.9; IR (ATR, cm^{-1}) $\tilde{\nu}$ = 750, 831, 868, 899, 966, 1007, 1063, 1072, 1101, 1144, 1169, 1248, 1263, 1393, 1587, 1722, 2905, 2959; HRMS (APPI): m/z calcd for $C_{44}H_{76}I_2O_{13}Si_6Na$: 1257.1883; found: 1257.1893 $[(M + Na)^+]$.

6,6'-Bis(*O*-4-pyren-1-ylethynylbenzoyl)- 2,3,4,2',3',4'-hexakis(*O*-trimethylsilyl)-α,α-trehalose (5a)

Under a nitrogen atmosphere, 1-ethynylpyrene (1.29 g, 4.32 mmol) was added into a solution of 6,6'-bis(*O*-4-iodobenzoyl)-2,3,4,2',3',4'-hexakis(*O*-trimethylsilyl)-α,α-trehalose **4** (1.33 g, 1.08 mmol), $PdCl_2(PPh_3)_2$ (151.3 mg, 0.216 mmol) and CuI (41.0 mg, 0.216 mmol) in triethylamine (27 mL) and THF (38 mL), and the mixture was stirred at room temperature for 48 h. After volatile materials were removed under reduced pressure, the residue was dissolved in CH_2Cl_2 (50 mL). The organic layer was washed with aqueous H_2O (10 mL × 3), and dried over Na_2SO_4. The crude mixture was purified by column chromatography on silica gel (*n*-hexane/EtOAc, 7:1). Further purification was also carried out by column chromatography on silica gel (toluene) to give 6,6'-bis(*O*-4-pyren-1-ylethynylbenzoyl)-2,3,4,2',3',4'-hexakis(*O*-trimethylsilyl)-α,α-trehalose **5a** as a yellow solid. Yield, 952.1 mg (0.663 mmol), 61%; mp, 219.5−220.5°C; ^{1}H NMR (500 MHz, $CDCl_3$) δ 0.18 (18H, s), 0.20 (18H, s), 0.22 (18H, s), 3.57 (2H, dd, *J* = 3.1 and 9.3 Hz), 3.70 (2H, t, *J* = 9.0 Hz), 4.03 (2H, t, *J* = 8.9 Hz), 4.18 (2H, dt, *J* = 2.6 and 9.4 Hz), 4.35 (dd, *J* = 3.8 and 11.8 Hz), 4.65 (dd, *J* = 2.4 and 11.8 Hz), 5.06 (2H, d, *J* = 3.0 Hz), 7.80 (4H, d, *J* = 8.2 Hz), 7.99−8.03 (4H, m), 8.08−8.21 (16H, m), 8.62 (2H, d, *J* = 9.1 Hz); ^{13}C NMR (125 MHz, $CDCl_3$) δ 0.31, 0.95, 1.11, 64.0, 70.9, 72.0, 72.8, 73.6, 91.9, 94.3, 94.5, 117.0, 124.2, 124.4, 124.5, 125.3, 125.7, 125.8, 126.3, 127.2, 128.4, 128.5, 129.4, 129.7, 129.8, 131.0, 131.2, 131.6 (2C), 132.0, 166.0; IR (ATR, cm^{-1}) $\tilde{\nu}$ = 715, 748, 764, 837, 870,

964, 1011, 1072, 1097, 1171, 1250, 1263, 1408, 1607, 1724, 2342, 2903, 2955, 3042; HRMS (APCI): m/z calcd for $C_{80}H_{95}O_{13}Si_6$: 1431.5383; found: 1431.5374 [$(M + H)^+$].

6,6'-Bis(*O*-4-anth-9-ylethynylbenzoyl)-2,3,4,2',3',4'-hexakis(*O*-trimethylsilyl)-α,α-trehalose (5b)

Under a nitrogen atmosphere, 9-ethynylanthracene (770.0 mg, 2.81 mmol) was added into a solution of 6,6'-bis(*O*-4-iodobenzoyl)-2,3,4,2',3',4'-hexakis-(*O*-trimethylsilyl)-α,α-trehalose **4** (860.4 mg, 1.08 mmol), $PdCl_2(PPh_3)_2$ (100.2 mg, 0.140 mmol) and CuI (30.1 mg, 0.140 mmol) in triethylamine (13 mL) and THF (20 mL), and the mixture was stirred at room temperature for 48 h. After volatile materials were removed under reduced pressure, the residue was dissolved in CH_2Cl_2 (50 mL). The organic layer was washed with aqueous H_2O (10 mL × 3), and dried over Na_2SO_4. The crude mixture was purified by column chromatography on silica gel (*n*-hexane/EtOAc, 7:1). Further purification was also carried out by column chromatography on silica gel (toluene) to give 6,6'-bis(*O*-4-anth-9-ylethynylbenzoyl)-2,3,4,2',3',4'-hexakis(*O*-trimethylsilyl)-α,α-trehalose **5b** as a yellow solid. Yield, 665.9 mg (0.480 mmol), 69%; mp, 145.5−146.5°C; ^{1}H NMR (500 MHz, $CDCl_3$) δ 0.19 (18H, s), 0.21 (18H, s), 0.22 (18H, s), 3.57 (2H, dd, *J* = 3.0 and 9.3 Hz), 3.71 (2H, t, *J* = 9.0 Hz), 4.03 (2H, t, *J* = 8.9 Hz), 4.20 (2H, d, *J* = 9.3 Hz), 4.36 (2H, dd, *J* = 3.4 and 12.0 Hz), 4.66 (2H, d, *J* = 12.0 Hz), 5.06 (2H, d, *J* = 2.9 Hz), 7.51 (4H, t, *J* = 8.2 Hz), 7.61 (4H, t, *J* = 8.6 Hz), 7.85 (4H, d, *J* = 7.7 Hz), 8.01 (4H, d, *J* = 8.4 Hz), 8.16 (4H, d, *J* = 7.9 Hz), 8.45 (2H, s), 8.62 (4H, d, *J* = 8.0 Hz); ^{13}C NMR (125 MHz, $CDCl_3$) δ 0.30, 0.94, 1.11, 63.9, 70.9, 72.0, 73.6, 76.7, 89.5, 94.6, 99.9, 116.5, 125.8, 126.5, 126.9, 128.4 (2C), 128.8, 129.4, 129.8, 131.1, 131.5, 132.7, 165.9; IR (ATR, cm^{-1}) $\tilde{\nu}$ = 735, 766, 831, 866, 934, 968, 1013, 1074, 1107, 1153, 1171, 1248, 1404, 1603, 1717, 2195, 2361, 2899, 2957, 3057; HRMS (APCI): m/z calcd for $C_{76}H_{95}O_{13}Si_6$: 1383.5310; found: 1383.5276 [$(M + H)^+$].

6,6'-Bis(*O*-4-phenylethynylbenzoyl)-2,3,4,2',3',4'-hexakis(*O*-trimethylsilyl)-α,α-trehalose (5c)

Under a nitrogen atmosphere, ethynylbenzene (183.4 mg, 1.80 mmol) was added into a solution of

6,6'-bis(*O*-4-iodobenzoyl)-2,3,4,2',3',4'-hexakis(*O*-trimethylsilyl)-α,α-trehalose **4** (740.4 mg, 0.60 mmol), $PdCl_2(PPh_3)_2$ (80.0 mg, 0.120 mmol) and CuI (20.1 mg, 0.120 mmol) in triethylamine (15 mL) and THF (21 mL), and the mixture was stirred at room temperature for 48 h. After volatile materials were removed under reduced pressure, the residue was dissolved in CH_2Cl_2 (50 mL). The organic layer was washed with aqueous H_2O (10 mL × 3), and dried over Na_2SO_4. The crude mixture was purified by column chromatography on silica gel (*n*-hexane/EtOAc, 7:1). Further purification was also carried out by column chromatography on silica gel (toluene) to give 6,6'-bis(*O*-4-phenylethynylbenzoyl)-2,3,4,2',3',4'-hexakis(*O*-trimethylsilyl)-α,α-trehalose **5c** as a white powder. Yield, 612.9 mg (0.520 mmol), 87%; mp, 154.5−155.5°C; ^{1}H NMR (500 MHz, $CDCl_3$) δ 0.14 (18H, s), 0.16 (18H, s), 0.19 (18H, s), 3.52 (2H, dd, *J* = 3.0 and 9.4 Hz), 3.65 (2H, t, *J* = 8.9 Hz), 3.99 (2H, t, *J* = 9.0 Hz), 4.14 (2H, dt, *J* = 3.2 and 9.1 Hz), 4.30 (2H, dd, *J* = 3.7 and 12.0 Hz), 4.59 (2H, dd, *J* = 2.3 and 12.0 Hz), 5.00 (2H, d, *J* = 3.1 Hz), 7.35−7.38 (6H, m), 7.54−7.56 (4H, m), 7.61 (4H, d, *J* = 8.6 Hz), 8.04 (4H, d, *J* = 8.6 Hz); ^{13}C NMR (125 MHz, $CDCl_3$) δ 0.27, 0.90, 1.08, 63.9, 70.8, 72.0, 72.7, 73.6, 88.6, 92.5, 94.6, 122.6, 128.1, 128.4, 128.8, 129.3, 129.6, 131.5, 131.7, 165.9; IR (ATR, cm^{-1}) $\tilde{\nu}$ = 756, 833, 868, 901, 943, 964, 1005, 1043, 1074, 1097, 1142, 1169, 1250, 1269, 1406, 1607, 1726, 2340, 2359, 2907, 2959; HRMS (APCI): m/z calcd for $C_{60}H_{86}O_{13}Si_6Na$: 1205.4576; found: 1205.4581 [$(M + Na)^+$].

6,6'-Bis(*O*-4-pyren-1-ylethynylbenzoyl)-α,α-trehalose (1a)

Under a nitrogen atmosphere, 1.0 M THF solution of tetrabutylammonium fluoride (1.15 mL, 1.15 mmol) was added into a solution of 6,6'-bis(*O*-4-pyren-1-ylethynylbenzoyl)-2,3,4,2',3',4'-hexakis(*O*-trimethylsilyl)-α,α-trehalose **5a** (229.8 mg, 0.160 mmol) in THF (23 mL) and methanol (16 mL), and the mixture was stirred at room temperature for 2 h. The solvents were removed under reduced pressure, the crude mixture was purified by column chromatography on silica gel (toluene/EtOAc/methanol, 2:2:1). Additional purification was carried out by column chromatography on florisil (EtOAc to EtOAc/methanol, 6:1) to give 6,6'-bis(*O*-4-pyren-1-ylethynylbenzoyl)-α,α-trehalose **1a** as a yellow solid. Yield, 83.9 mg (84.0 μmol), 52%; mp,

185−186°C; ^{1}H NMR (500 MHz, DMSO d_6) δ 3.33−3.37 (2H, m), 3.43−3.47 (2H, m), 3.66−3.71 (2H, m), 4.18−4.21 (2H, m), 4.39−4.43 (2H, m), 4.52 (2H, d, J = 10.7 Hz), 5.00 (2H, d, J = 3.8 Hz), 5.09 (2H, d, J = 5.9 Hz), 5.11 (2H, d, J = 4.6 Hz), 5.32 (2H, d, J = 5.2 Hz), 7.86 (4H, d, J = 8.2 Hz), 8.05 (4H, d, J = 8.2 Hz), 8.06 (2H, d, J = 7.4 Hz), 8.12 (2H, d, J = 9.0 Hz), 8.19−8.23 (6H, m), 8.27−8.30 (6H, m), 8.54 (2H, d, J = 9.1 Hz); ^{13}C NMR (125 MHz, DMSO d_6) δ 64.4, 69.9, 70.2, 71.5, 72.9, 91.3, 94.0, 94.3, 116.0, 123.3, 123.5, 124.7, 124.9, 126.08, 126.13, 126.7, 127.1, 128.56, 128.62, 128.99, 129.6 (2C), 129.8, 130.4, 130.7, 131.25, 131.29, 131.8, 165.1; IR (ATR, cm^{-1}) $\tilde{\nu}$ = 718, 766, 845, 984, 1016, 1045, 1074, 1126, 1175, 1269, 1377, 1445, 1605, 1713, 2342, 2876, 2945, 2959, 3312 (br); HRMS (APPI): m/z calcd for $C_{62}H_{46}O_{13}Cl$: 1033.2632; found: 1033.2679 [(M + Cl)$^-$].

6,6'-Bis(*O*-4-anth-9-ylethynylbenzoyl)-*α*,*α*-trehalose (1b)

Under a nitrogen atmosphere, 1.0 M THF solution of tetrabutylammonium fluoride (1.44 mL, 1.44 mmol) was added into a solution of 6,6'-bis(*O*-4-anth-9-ylethynylbenzoyl)-2,3,4,2',3',4'-hexakis(*O*-trimethylsilyl)-*α*,*α*-trehalose **5b** (186.2 mg, 0.140 mmol) in THF (20 mL) and methanol (14 mL), and the mixture was stirred at room temperature for 2 h. The solvents were removed under reduced pressure, the crude mixture was purified by column chromatography on florisil (EtOAc to EtOAc/methanol, 6:1) to give 6,6'-bis(*O*-4-anth-9-ylethynylbenzoyl)-*α*,*α*-trehalose **1b** as an orange color solid. Yield, 40.6 mg (42.7 μmol), 31%; mp, 230−231°C; ^{1}H NMR (500 MHz, DMSO d_6) δ 3.29−3.33 (2H, m), 3.41−3.45 (2H, m), 3.66 (2H, sep, J = 4.6 Hz), 4.18−4.21 (2H, m), 4.39 (2H, q, J = 5.9 Hz), 4.51 (2H, d, J = 10.3 Hz), 4.97 (2H, d, J = 3.5 Hz), 5.07 (4H, t, J = 5.6 Hz), 5.29 (2H, d, J = 5.6 Hz), 7.58 (4H, t, J = 7.9 Hz), 7.68 (4H, t, J = 6.8 Hz), 7.98 (4H, d, J = 8.3 Hz), 8.08 (4H, d, J = 8.3 Hz), 8.14 (4H, d, J = 8.6 Hz), 8.56 (4H, d, J = 8.8 Hz), 8.70 (2H, s); ^{13}C NMR (125 MHz, DMSO d_6) δ 64.5, 69.9, 70.2, 71.5, 72.9, 88.7, 94.0, 99.9, 115.1, 125.9, 126.1, 127.2, 127.7, 128.7, 128.9, 129.0, 129.6, 130.7, 131.9, 132.0, 165.2; IR (ATR, cm^{-1}) $\tilde{\nu}$ = 725, 764, 841, 880, 945, 988, 1015, 1065, 1107, 1136, 1179, 1281, 1329, 1406, 1605, 1697, 2361, 2914, 3418 (br); HRMS (APPI): m/z calcd for $C_{58}H_{46}O_{13}Cl$: 985.2632; found:

985.2666 [(M + Cl)$^-$].

6,6'-Bis(*O*-4-phenylethynylbenzoyl)-α,α-trehalose (1c)

Under a nitrogen atmosphere, 1.0 M THF solution of tetrabutylammonium fluoride (1.99 mL, 1.99 mmol) was added into a solution of 6,6'-bis(*O*-4-phenylethynylbenzoyl)-2,3,4,2',3',4'-hexakis*O*-(trimethylsilyl)-α,α-trehalose **5c** (249.9 mg, 0.210 mmol) in THF (30 mL) and methanol (21 mL), and the mixture was stirred at room temperature for 2 h. The solvents were removed under reduced pressure, the crude mixture was purified by column chromatography on florisil (EtOAc to EtOAc/methanol, 6:1) to give 6,6'-bis(*O*-4-phenylethynylbenzoyl)-α,α-trehalose **1c** as an orange color solid. Yield, 74.0 mg (98.6 μmol), 47%; mp, 204.5−205.5°C; ^{1}H NMR (500 MHz, DMSO d_6) δ 3.24−3.31 (2H, m), 3.33−3.40 (2H, m), 3.61 (2H, sep, J = 6.1 Hz), 4.10−4.14 (2H, m), 4.32−4.37 (2H, m), 4.43 (2H, d, J = 13.3 Hz), 4.88 (2H, d, J = 4.5 Hz), 5.02−5.04 (4H, m), 5.25 (2H, d, J = 6.7 Hz), 7.43−7.44 (6H, m), 7.58 (4H, dd, J = 4.7 and 7.3 Hz), 7.69 (4H, d, J = 10.7 Hz), 7.98 (4H, d, J = 10.7 Hz); ^{13}C NMR (125 MHz, DMSO d_6) δ 64.3, 69.8, 70.1, 71.4, 72.9, 88.5, 92.3, 94.0, 121.7, 127.0, 128.9, 129.3, 129.5 (2C), 131.6, 131.7, 165.1; IR (ATR, cm^{-1}) $\tilde{\nu}$ = 754, 804, 856, 935, 984, 1016, 1043, 1076, 1142, 1177, 1271, 1406, 1441, 1607, 1715, 2365, 2941, 3298 (br); HRMS (APPI): m/z calcd for $C_{42}H_{38}O_{13}Cl$: 785.2006; found: 785.2043 [(M + Cl)$^-$].

Cellular Imaging Study

HeLa CD4$^+$ cells were grown on culture slides (96-well plate) and treated with 10% fetal bovine serum, penicillin and streptomycin at 37°C. Under 5% CO_2 atmosphere, 10μL of **1a** solution (0.75 to 37.5 μM in DMSO/PBS (80/20)) was added to the HeLa CD4$^+$ cells on D-MEM medium and incubated. After 90 min, the HeLa CD4$^+$ cells were washed with D-MEM medium two times, then the new medium (100μL) was added, and incubated. After 18 h, the cells were washed with PBS (100μL) for two times. The cells were subsequently analyzed using a filter

(>488 nm) on a BZ-8000 fluorescence microscope (KEYENCE, Japan).

Acknowledgements

We thank Mr. Takeshi Akimoto and Mr. Shinji Kawaguchi of Chiba Institute of Technology for measurements of the NMR spectroscopy and high resolution mass spectrometry. We are also grateful to Prof. Dr. Shin-ichiro Kato of The University of Shiga Prefecture for useful discussions with respect to the photophysical properties of trehalose-besed fluorescent probes.

References.

1. For recent book and reviews, see; (a) A. Mishra, P. Bäuerle *Angew. Chem., Int. Ed.* **2012**, *51*, 2020−2067. (b) S. Günes, H. Neugebauer, N. S. Sariciftci, *Chem. Rev.* **2007**, *107*, 1324–1338. (c) P. Cheng, X. Zhan, *Chem. Soc. Rev.* **2016**, *45*, 2544–2582. (d) V. Balzani, A. Credi, M. Venturi, *Molecular Devices and Machines*; Wiley-VCH: New York **2004**; Chapter 6.
2. For recent reviews, see; (a) H. Jiang *Asian J. Org. Chem.* **2014**, *3*, 102−112. (b) D. Li, H. Zhang, Y. Wang, *Chem. Soc. Rev.* **2013**, *42*, 8416−8433. (c) S. Chen, Q. Wu, M. Kong, X. Zhao, Z. Yu, P. Jia, W. J. Huang *Mater. Chem. C* **2013**, *1*, 3508−3524. (d) M. Zhu, C. Yang *Chem. Soc. Rev.* **2013**, *42*, 4963−4976.
3. For selected reviews, see; (a) C.-C. Shih, W.-Y. Lee, W.-C. Chen, *Mater. Horiz.* **2016**, *3*, 294–308. (b) J. E. Anthony, *Chem. Rev.* **2006**, *106*, 5028–5048. (c) C. Wang, H. Dong, W. Hu, Y. Liu, D Zhu, *Chem. Rev.* **2012**, *112*, 2208–2267.
4. For examples, see: (a) S. Shanmugaraju, P. S. Mukherjee *Chem. Commun.* **2015**, *51*, 16014−16032. (b) S. Toyota, T. Kawakami, T. Iwanaga *Synthesis* **2014**, *46*, 1667–1673. (c) S. Toyota, S. Karashima, T. Iwanaga *Bull. Chem. Soc. Jpn.* **2015**, *88*, 192−199. (d) Y. Niko, S. Kawauchi, S. Otsu, K. Tokumaru,

G.-i. Konishi *J. Org. Chem.* **2013**, *78*, 3196−3207. (e) T. H. El-Assaad, M. Auer, R. Castañeda, K. M. Hallal, F. M. Jradi, L. Mosca, R. S. Khnayzer, D. Patra, T. V. Timofeeva, J.-L. Brédas, E. J. W. List-Kratochvil, B. Wex, B. R. Kaafarani *J. Mater. Chem. C* **2016**, *4*, 3041−3058. (f) Wei-Jie Chi, Dao-Yuan Zheng, Xiao-Fang Chen Ze-Sheng Li *J. Mater. Chem. C* **2017**, *5*, 10055−10060.

5. P. Sam-ang, D. Raksasorn, M. Sukwattanasinitt, P. Rashatasakhon *RSC Adv.* **2014**, *4* , 58077–58082.
6. For similar example, the emitting properties of large π-conjugated compounds have also been used for the chemical detection, see; G. R. C. Hamilton, S. K. Sahoo, S. Kamila, N. Singh, N. Kaur, B. W. Hyland, J. F. Callan *Chem. Soc. Rev.* **2015**, *44*, 4415–4432.
7. N. Zhao, S. Xuan, Z. Zhou, F. R. Fronczek, K. M. Smith, M. G. H. Vicente *J. Org. Chem.* **2017**, *82*, 9744−9750.
8. For selected reviews, see; (a) D. Andina, J.-C. Leroux, P. Luciani *Chem. Eur. J.* **2017**, *55*, 13549–13573. (b) N. Gupta, S. I. Reja, V. Bhalla, M. Kumar *Org. Biomol. Chem.* **2017**, *15*, 6692–6701. (c) T. Ikeno, T. Nagano, K. Hanao *Chem. Asian J.* **2017**, *12*, 1435–1446. (d) Long Yi, Zhen Xi *Org. Biomol. Chem.* **2017**, *15*, 3828–3839. (e) J.-T. Hou, W. X. Ren, K. Li, J. Seo, A. Sharma, X.-Q. Yu, J. S. Kim *Chem. Soc. Rev.* **2017**, *46*, 2076−2090. (f) A. C. Bhasikuttan, J. Mohanty *Chem. Commun.* **2017**, *53*, 2789−2809.
9. S. T. Laughlin, J. M. Baskin, S. L. Amacher, C. R. Bertozzi *Science* **2008**, *320*, 664–667.
10. T.-L. Hsu, S. R. Hanson, K. Kishikawa, S.-K. Wang, M. Sawa, C.-H. Wong *Proc. Natl. Acad. Sci.* **2007**, *104*, 2614–2619.
11. A. Barattucci, E. Deni, P. Bonaccorsi, M. G. Ceraolo, T. Papalia, A. Santoro, M. T. Sciortino, F. Puntoriero *J. Org. Chem.* **2014**, *79*, 5113−5120.
12. E. Deni, A, Zamarrón, P. Bonaccorsi, M. C. Carreño, Á. Juarranz, F. Puntoriero, M. T. Sciortino, M. Ribagorda, A. Barattucci *Eur. J. Med. Chem.* **2016**, *111*, 58−71.

13. S. Ohtake, Y. J. Wang, *J. Pharm. Sci.* **2011**, *100*, 2020–2053.

14. (a) U. Pässler, M. Gruner, S. Penkov, T. V. Kurzchalia, H.-J. Knölker *Synlett* **2011**, *17*, 2482–2486. (b) V. A. Sarpe, S. S. Kulkarni *J. Org. Chem.* **2011**, *76*, 6866–6870.

15. A. Khan, K. Kodar, M. S. M. Timmer, B. L. Stocker *Tetrahedron* **2018**, *74*, 1269–1277.

16. (a) S.-W. Yang, A. Elangovan, K.-C. Hwang, T.-I. Ho *J. Phys. Chem. B* **2005**, 109, 16628–16635. (b) F. Zhong, J. Zhao *Dye. Pigm.* **2017**, *136*, 909–918.

17. The amphiphilic molecules having the pyrenyl group as a hydrophobic moiety can be self-assembled via hydrogen bond of hydrophilic moieties and π–π interaction between pyrenyl groups. C. Madhu, B. Roy, P. Makam, T. Govindaraju *Chem. Commun.* **2018**, *54*, 2280−2283.

18. All calculations were performed using: Gaussian 09, Revision B.01, M. J. Frisch, G. W. Trucks, H. B. Schlegel, G. E. Scuseria, M. A. Robb, J. R. Cheeseman, G. Scalmani, V. Barone, B. Mennucci, G. A. Petersson, H. Nakatsuji, M. Caricato, X. Li, H. P. Hratchian, A. F. Izmaylov, J. Bloino, G. Zheng, J. L. Son-nenberg, M. Hada, M. Ehara, K. Toyota, R. Fukuda, J. Hasegawa, M. Ishida, T. Nakajima, Y. Honda, O. Kitao, H. Nakai, T. Vreven, J. A. Montgomery, Jr., J. E. Peralta, F. Ogliaro, M. Bearpark, J. J. Heyd, E. Brothers, K. N. Kudin, V. N. Staroverov, R. Kobayashi, J. Normand, K. Raghavachari, A. Rendell, J. C. Burant, S. S. Iyengar, J. Tomasi, M. Cossi, N. Rega, J. M. Millam, M. Klene, J. E. Knox, J. B. Cross, V. Bakken, C. Adamo, J. Jaramillo, R. Gomperts, R. E. Stratmann, O. Yazyev, A. J. Austin, R. Cammi, C. Pomelli, J. W. Ochterski, R. L. Martin, K. Morokuma, V. G. Zakrzewski, G. A. Voth, P. Salvador, J. J. Dannenberg, S. Dapprich, A. D. Daniels, Ö. Farkas, J. B. Foresman, J. V. Ortiz, J. Cioslowski, D. J. Fox, Gaussian, Inc., Wallingford CT, 2010.

19. A. D. Becke *J. Chem. Phys.*, **1993**, 5648−5652.

20. C. Lee, W. Yang, R. G. Parr *Phys. Rev. B*, **1988**, *37*, 785−789.

21. B. Miehlich, A. Savin, H.Stoll, H. Preuss *Chem. Phys. Lett.*, **1989**, *157*, 200−206.

22. J. C. Jiang, Y. S. Wang, H. C. Chang, S. H. Lin, Y. T. Lee, G. Niedner-Schatteburg, H. C. Chang, *J. Am. Chem. Soc.* **2000**, *122*, 1398−1410.

23. J. T. H. Dunning *J. Chem. Phys.* **1989**, *90*, 1007−1023.

24. Y.-Y. Chen, H. Wang, D.-W. Zhang, J.-L. Hou, Z.-T. Li *Chem. Commun.* **2015**, *51*, 12088−12091.